JOURNAL OF CATALYSIS 151, 155–167 (1995)

The Effect of Chloride Ions on a Li^+–MgO Catalyst for the Oxidative Dehydrogenation of Ethane

Dingjun Wang, Michael P. Rosynek, and Jack H. Lunsford[1]

Department of Chemistry, Texas A&M University, College Station, Texas 77843

Received May 5, 1994; revised September 21, 1994

The addition of chloride ions to a Li^+–MgO catalyst at a ratio of Cl/Li ≥0.9 significantly improves the yields of ethylene that can be achieved during the oxidative dehydrogenation (OXD) of ethane. At 620°C, C_2H_4 yields of 58% (75% conversion, 77% selectivity) have been maintained for up to 50 h on stream. These ethylene yields are consistent with the large C_2H_4/C_2H_6 ratios that are attained over these catalysts during the oxidative coupling of CH_4. The activity of the catalysts with Cl/Li ≥0.9 is partly a result of the fact that CO_2 formed during the reaction does not poison the catalyst. In addition, the surface areas of the chlorided catalysts are greater than those which contain a comparable amount of Li, but no chloride ions. Based upon the activity results, CO_2 temperature-programmed desorption data, and X-ray photoelectron spectra, a model has been proposed in which lithium is mainly present as LiCl on the MgO support, provided a nearly stoichiometric amount of chloride is available. The active centers are believed to be associated with a thin (atomic) layer of Li_2O that partially covers the LiCl crystallites. This Li_2O is capable of activating C_2H_6, but its basic strength has been modified so that it does not form carbonate ions at 620°C. When the amount of chloride is limited, or is not present at all, multilayers of more strongly basic Li_2O form on the surface of LiCl and/or on the MgO. In the presence of CO_2, this Li_2O is extensively converted to Li_2CO_3, which is inactive for the OXD reaction. © 1995 Academic Press, Inc.

INTRODUCTION

It was previously demonstrated that the addition of chloride ions to a Li^+–MgO catalyst significantly increased the yield of ethylene during the oxidative dehydrogenation (OXD) of ethane (1). This promotional effect of chloride ions has consequences during the oxidative coupling of methane in that the resulting C_2H_4/C_2H_6 product ratios are much greater than those obtained over a chloride-free Li^+–MgO catalyst at comparable levels of conversion (2, 3). Moreover, as pointed out by Burch and Crabb (4), among those catalysts that they considered for the OXD of C_2H_6, only Li^+–MgO–Cl^- exhibited ethylene yields which exceeded those attained in a noncatalyzed reaction under optimum conditions. One of the more significant features of the Li^+–MgO–Cl^- catalyst is that it is sufficiently active that it can be used at $T \leq 650$°C, which means that the loss of chlorine from the catalyst is slow, and the secondary homogeneous oxidation of the product C_2H_4 is minimized. By adding certain lanthanide oxides (e.g., Dy_2O_3) to the catalyst, it is possible to increase the activity even further, without sacrificing selectivity, so that the OXD reaction can be carried out at temperatures as low as 570°C (5).

In the present study, the role of chloride ions in improving properties of the Li^+–MgO catalyst for the OXD of ethane was investigated in more detail, with attention being given to the near-surface composition of the catalyst. Kinetic results provide additional information on the reaction mechanism. Moreover, the significance of surface chloride ions relative to gas-phase chlorine is addressed further. These results are compared with those recently obtained for the oxidative coupling of methane over a similar set of catalysts (3).

EXPERIMENTAL

Catalyst. In the previous study (1), chloride ions were introduced into the catalyst during the formation of a sol–gel by the addition of NH_4Cl to a slurry of MgO or by the reaction of gas phase HCl with a Li^+–MgO material. We have found, however, that some of the most active and selective catalysts can be prepared by adding aqueous HCl to a slurry of MgO, followed by the addition of a solution of $LiNO_3$. In particular, MgO powder (Fisher "light", M-349-4, 98% pure) was added to 200 ml of deionized water in a 500 ml, 3-neck round-bottom flask, equipped with an addition funnel and a water-cooled condenser. It is important that the MgO be of low apparent density. The behaviors of catalysts prepared using MgO of high apparent density were inferior and irreproducible. The slurry was kept at approximately 65°C, with constant stirring. A solution of HCl in 100 to 200 ml of deionized water was slowly added to the slurry

[1] To whom correspondence should be addressed.

0021-9517/95 $6.00

over a 1 to 2 h period. By varying the amount of HCl, the final chlorine content of the catalyst could be modified. After ca. 24 h at 65°C, a 100 ml solution of $LiNO_3$ was added. The slurry was transferred to a 3-l beaker, and the water was slowly evaporated during continuous stirring. The material was dried in air at 130–150°C and the resulting solid was ground into a powder. The catalyst was then calcined in air at 500°C for 1.5 h and at 750°C for 16 h, cooled in air to 150°C, and rapidly transferred to a glove box. In the glove box, the sample was crushed, sieved to 20/45 mesh size, and sealed in a bottle. The chlorided catalysts were stored in a desiccator because they were hygroscopic. The catalysts are designated as Li^+–MgO–Cl^- (A/B), where A and B refer to the atomic ratio of Li^+ and Cl^- with respect to Mg^{2+}. The standard Li^+–MgO catalysts were prepared from a slurry of Li_2CO_3 and MgO, as described previously (6). They are designated Li^+–MgO (*C*), where *C* refers to the atomic ratio of Li^+ to Mg^{2+} ions.

Reactor system. Reactions were carried out in both integral and differential modes. The integral reactor was constructed of a high-purity alumina tube (Coors, 99.8% Al_2O_3) that had an I.D. of 19 mm at its inlet end and 3 mm at its exit. A stainless-steel reactor cap, constructed from a modified Swagelock union tree, accommodated a high-purity alumina thermocouple well (Coors) that extended into the catalyst bed. The reactor was heated by a split furnace. The space between the reactor and the furnace was filled with molecular sieve to reduce thermal gradients. The amount of catalyst used in the integral reactor, unless indicated otherwise, was 5.2 g. Alumina chips were placed above the catalyst bed. The reactor and the alumina chips were routinely washed with HNO_3 when the catalyst was changed. The differential reactor, which was constructed from an alumina tube having an i.d. of 6.4 mm (Coors, 99.8% Al_2O_3), was used in the kinetic experiments. To minimize the contribution from any non-catalytic reactions, quartz chips were placed above and below the catalyst bed. A thermocouple in a small alumina tube was attached to the outside wall of the reactor. The volume of the catalyst was 1.0 ml, unless specified otherwise.

Reactant and diluent gases, C_2H_6 (99.5%), O_2 (extra dry), 10% N_2 in He, and CO_2 (99.5%) were obtained from Matheson and were used without further purification. Gas flows were regulated by mass flow controllers (MKS Model 1159A). The N_2 was used as an internal standard. Reaction mixtures were analyzed using a gas chromatograph (HP5890A), equipped with a Spherocarb column. The catalyst in the reactor was heated to 580–620°C in flowing N_2/He and then in O_2 for 4 h before admission of ethane and oxygen. All studies were carried out at atmospheric pressure, an ethane pressure of 290 Torr, and a C_2H_6/O_2 ratio of unity unless indicated otherwise.

Catalyst characterization. At the reactor outlet, two water traps, cooled to 0°C, were used to remove evolved HCl and most of the product H_2O from the exit gas stream. The chlorine concentration in the solution was measured periodically using a chloride test kit (La Motte Chemical). The chlorine contents of fresh and used catalysts were determined gravimetrically using $AgNO_3$. Inductively coupled plasma (ICP) analysis was used to determine the Li and Mg contents of the catalyst.

Surface analyses were performed with a Perkin-Elmer (PHI) Model 5500 X-ray photoelectron spectrometer. Before obtaining XPS data, the catalysts were treated in one of two ways: (i) The samples designated "fresh" were prepared by returning the previously calcined samples to the glove box for the preparation of a wafer. The wafer was then transferred to the spectrometer in a sealed vessel and was introduced without exposure to the air. (ii) Used catalyst samples were prepared in a similar manner, except that after treatment under reaction conditions, the reactor was sealed, and the sample was unloaded in the glove box. Prior to sealing the reactor, the catalyst was cooled quickly in a flow of O_2, He and CO_2. Peaks were deconvoluted and fitted to a Gaussian shape function. Peak areas were converted into atomic compositions using appropriate photoionization cross sections. Binding energies are referenced to the carbon 1s line of adventitious carbon at 284.6 eV.

Temperature-programmed desorption of CO_2 was carried out in an alumina reactor that typically contained 0.1 g of catalyst. The catalyst was pretreated in situ by heating in flowing He (50 ml/min) for 2 h at 750°C. The catalyst was then heated in the presence of a flowing CO_2/He mixture (CO_2/He = 0.66, 50 ml/min) for 2 h at 600°C and cooled in the presence of CO_2 to 120°C. After purging the system with He at 120°C for 30 min, the sample was heated in flowing He (30 ml/min) at a constant rate of 16°C/min to either 870°C or 950°C and then maintained at that temperature for an additional 30 min. The CO_2 that desorbed was determined using a thermal conductivity detector. A mass spectrometer attached to the outlet confirmed that only CO_2 evolved from the samples.

RESULTS AND DISCUSSION

Effect of Cl/Li ratio on the OXD of ethane. The compositions of a series of catalysts are given in Table 1. The nominal compositions were determined from the amounts of the various components used in the preparation of the catalysts. It is apparent that the Li/Mg ratio remained almost constant after calcination at 750°C in air, but the amount of chlorine lost strongly depended on the initial Cl/Li ratios in the catalysts. If the Cl/Li atomic ratio prior to calcination was >1, then chlorine was lost until the ratio decreased to ca. 0.9 to 1.0; if the original

TABLE 1

Effect of Calcination and Reaction on the Catalyst Composition and Surface Area

Atomic ratio						Surface area (m^2/g)	
Nominal		After calcination		After use[a]			
Li/Mg/Cl	Cl/Li	Li/Mg/Cl	Cl/Li	Li/Mg/Cl	Cl/Li	Fresh	Used
0.53/1/1.05	2.0	0.46/1/0.45	0.98	nd[b]	nd	1.3	nd
0.46/1/0.69	1.5	0.44/1/0.42	0.95	nd	nd	1.5	1.6
0.14/1/0.21	1.5	0.18/1/0.16	0.89	0.10/1/0.09	0.90	1.3	1.7
0.34/1/0.34[c]	1.0	0.37/1/0.33	0.88	0.28/1/0.10[d]	0.36	1.2	1.9
0.37/1/0.37	1.0	0.41/1/0.37	0.91	nd	nd	2.8	3.3
0.36/1/0.31	0.86	0.40/1/0.33	0.83	0.36/1/0.29	0.79	1.8	2.6
0.36/1/0.22	0.61	0.37/1/0.24	0.65	0.37/1/0.24	0.65	0.87	1.0
0.037/1/0.21	5.7	0.044/1/0.042	0.95	0.026/1/0.019	0.73	3.3	nd
0.0068/1/0.20	29	nd	nd	nd	nd	2.7	2.9
0.39/1/0	0.0	0.54/1/0	0	nd	nd	0.52	0.50
0.03/1/0	0.0	0.028/1/0	0	nd	nd	3.6	2.9

[a] Samples were used in the reaction for about 50 h in the integral reactor.
[b] Not determined.
[c] Sample prepared by addition of LiCl to MgO.
[d] The sample was used in the reaction for 550 h in the integral reactor.

ratio was ≤ 1 very little chlorine was lost. A sample that was prepared with HCl, but without lithium, lost all of its chlorine during calcination. These results indicate that magnesium chloride or oxychloride is unstable under calcination conditions and that the chloride ions are mainly associated with lithium ions. The presence of crystalline LiCl in these catalysts has been confirmed by X-ray diffraction (3).

It should also be noted from the results in Table 1 that the sample containing a substantial amount of lithium, but no chlorine (Li^+–MgO (0.39)), had a low surface area after calcination, whereas, those with Cl/Li ratios near unity had surface areas three to five times greater. A larger surface area also was found for the sample having a much smaller amount of lithium (Li^+–MgO (0.03)). Thus, lithium promotes sintering of the MgO while chloride ions inhibit this effect.

The additional effect of chlorine incorporation on the OXD of ethane is shown in Fig. 1. These catalysts all contained 4.5–5.0 wt% Li. Clearly, the maximum ethane conversion was observed at a nominal ratio of Cl/Li $\simeq$ 1. The conversion level decreased from its maximum at 80% to a level of only 10% as the Cl/Li ratio decreased to 0.65. Similar effects were observed previously for the C_2H_4/C_2H_6 ratio during the oxidative coupling of CH_4 (3). That is, large C_2H_4/C_2H_6 ratios were attained only when the Cl/Li ratio of the catalyst approached unity.

Surprisingly, during the OXD of C_2H_6, the selectivity for C_2H_4 remained nearly constant for all of the catalysts, even though the conversion levels varied significantly. This result suggests that as the Cl/Li ratio increases the rate constant for C_2H_4 conversion to CO_x decreases. Chloride ions must function as a poison for nonselective sites (see below).

The results of Fig. 2 demonstrate the stability of selected catalysts with respect to time on stream. The Li^+–MgO–Cl^- (0.36/0.22) catalyst with Cl/Li $\leq$ 0.9 exhibited

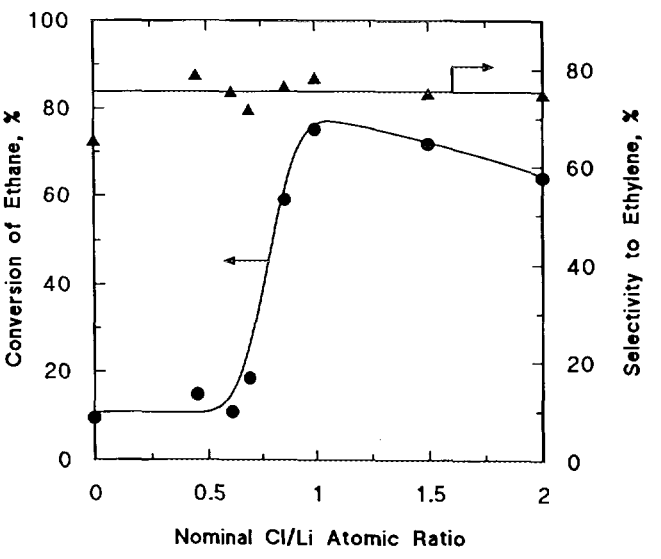

FIG. 1. Effect of nominal Cl/Li ratio on the activity and selectivity for the OXD of ethane in the integral reactor. The catalysts contained 4.5–5.0 wt% Li. Data were taken with 5.2 g catalyst at 620°C after ca. 15 h on stream.

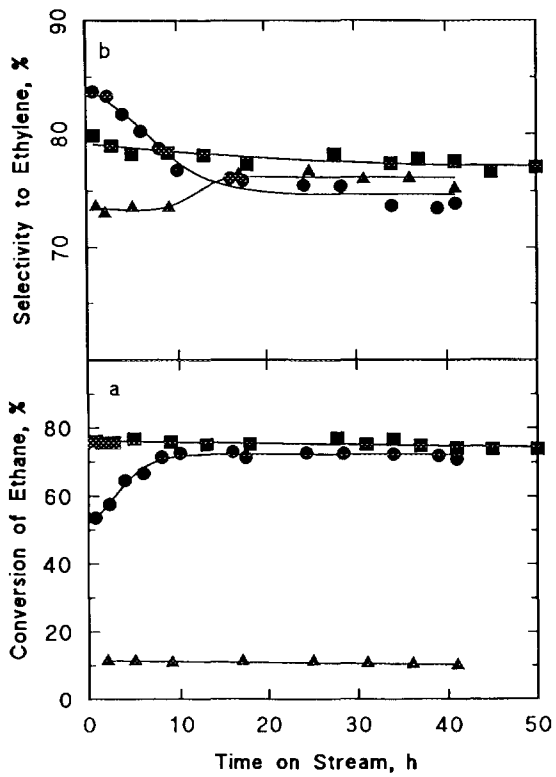

FIG. 2. The OXD of ethane as a function of time on stream in the integral reactor: (a) conversion and (b) selectivity. $P(C_2H_6)$ = 290 Torr, $P(O_2)$ = 290 Torr, T = 620°C, total flow rate = 60 ml/min. ■, Li^+–MgO–Cl^- (0.37/0.37); ●, Li^+–MgO–Cl^- (0.46/0.69); △, Li^+–MgO–Cl^- (0.36/0.22).

reasonably stable activity throughout the entire time period, whereas, the Li^+–MgO–Cl^- (0.46/0.69) catalyst with Cl/Li = 0.95 after calcination was characterized by an initial increase in conversion and a decrease in selectivity. These transient effects may reflect the loss of a small amount of chlorine, such that the Cl/Li ratio approaches as ideal value of 0.9, or they may result from a redistribution of Li and Cl on the surface. It may be necessary that a small fraction of the Li be free to interact with oxygen or with the MgO in order to generate active centers (see below). The C_2H_4 yield of 58%, obtained with the Li^+–MgO–Cl^- (0.37/0.37) catalyst, is remarkable, particularly since it remained stable for 50 h.

Additional studies were carried out on catalysts which had either different *total* amounts of lithium and chlorine, with a Cl/Li ratio near unity, or had a Cl/Li ratio significantly less than unity. The results demonstrate that the Cl/Li ratio is a much more important factor in determining the C_2H_6 conversion than is the absolute amounts of Cl and Li. For example, the catalyst Li^+–MgO–Cl^- (0.037/0.21) was more active, and even more selective, than the Li^+–MgO–Cl^- (0.36/0.22) catalyst. But catalysts containing more Cl and Li were stable over long periods on stream. The C_2H_6 conversion over the Li^+–MgO–Cl^- (0.0068/0.20) catalyst, for example, decreased from nearly 60 to only 20% over 40 h on stream. Apparently, the excess Li and Cl serve as a reservoir for promoters that are lost during the reaction.

One catalyst was prepared by adding LiCl to MgO (Li^+–MgO–Cl^- (0.34/0.34)). This was followed by the usual calcination at 750°C. The conversion and selectivity over this material were obtained for a period of 520 h. Under the usual operating conditions (T = 620°C, 60 ml/min, 5.2 g catalyst), the C_2H_6 conversion increased from 54 to 85% over a period of 13 h, and then decreased to 50% over the remaining 500 h. Meanwhile, the C_2H_4 selectivity decreased from 82 to 73%, and then slowly increased to 78%. In view of the fact that the final catalyst had a Cl/Li ratio of only 0.36, it is surprising that the conversion level was as large as 50%.

The loss of chlorine from the catalysts in the integral reactor is summarized in Table 2. In general, the rate of

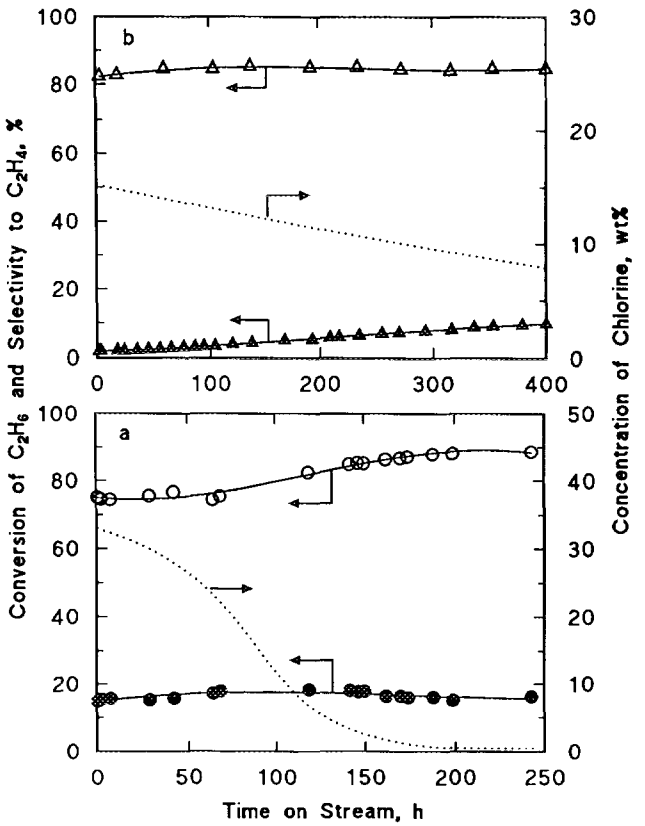

FIG. 3. The OXD of ethane as a function of time on stream in the differential reactor (T = 620°C, $P(C_2H_6)$ = 290 Torr, $P(O_2)$ = 290 Torr, total flow rate = 60 ml/min, 1.0 ml catalyst): conversion and selectivity over (a) Li^+–MgO–Cl^- (0.46/0.69) and (b) Li^+–MgO–Cl^- (0.36/0.22). The dotted line refers to the amount of chlorine remaining in the catalyst.

TABLE 2

Conversion and Evolution of Chlorine

Catalyst	Time on stream (h)	Conversion (%)	Cl evolution (μmol/h)	Cl content (wt%)	C_2H_4/Cl (atomic ratio)
Li^+–MgO–Cl^- (0.46/0.69)	0			25.3	
	16	68	244[a]	22.6	223[b]
	41	72	99.8	20.9	
Li^+–MgO–Cl^- (0.34/0.34)	0			21.4	
	19	72	231	18.4	241
	43	77	108	16.6	
Li^+–MgO–Cl^- (0.37/0.37)	0			22.1	
	18	76	160	20.1	301
	43	75	99.6	18.4	
Li^+–MgO–Cl^- (0.037/0.21)	0			3.5	
	26	69	83.4	2.0	
	32	64	34.8	1.9	614
	44	61	24.7	1.7	
	50	59	23.5	1.6	
Li^+–MgO–Cl^- (0.36/0.22)	0			15.2	
	14	12	16	15.1	379
	41	11	12	14.7	
	2.3[c]	12	199	14.9	

[a] Average data during the period specified; for example, 0–16 h on stream.
[b] Average data through the entire time on stream.
[c] Water added at a rate of 3.7 g/h in the separate experiment.

chlorine evolution was larger at shorter times on stream, but even after 40–50 h less than 25% of the chlorine has been lost from the catalysts. By operating under differential conditions, however, it was possible to accelerate the loss of chlorine. Presumably, secondary reaction with the evolved HCl did not occur as efficiently at the larger space velocities used in the differential reactor. As shown in Fig. 3a the rate of chlorine loss and the total chlorine content decreased to almost zero for the Li^+–MgO–Cl^- (0.46/0.69) catalyst after 175 h on stream. By contrast, after 400 h of use the Cl^- content of the Li^+–MgO–Cl^- (0.36/0.22) catalyst decreased to only about 50% of its initial level because the rate of chlorine loss was less (Fig. 3b). This difference in rates of chlorine loss may be attributed to the larger rate of reaction, and hence H_2O formation, over the Li^+–MgO–Cl^- (0.46/0.69) catalyst. Water is known to be a contributing factor in the loss of chlorine from these catalysts (1, 7).

The conversion data reported in Fig. 3 appear to contradict the earlier point that Cl/Li ratios $\geq$0.9 are required for high OXD activity. The results of Fig. 3a show that during the first 150 h of operation the activity of the Li^+–MgO–Cl^- (0.46/0.69) catalyst increased slightly, even though the Cl/Li ratio became quite small. By contrast, the activity of the Li^+–MgO–Cl^- (0.36/0.22) catalyst initially was small, but continued to increase over 400 h. At the end of the experiments, the activities of the two catalysts were comparable (15% conversion vs 10% conversion). As will be discussed in more detail below, a major impediment to achieving high activity with the Li^+–MgO–Cl^- (0.36/0.22) catalyst is the fact that the surface is partially covered by Li_2CO_3, which appears to be inactive for the OXD reaction (8). One of the roles of chlorine is to fix lithium as LiCl and to prevent the formation of carbonate, which may spread over the surface during calcination at 750°C. (The melting point of Li_2CO_3 is 723°C.) Once this function is achieved, the Li_2CO_3 does not spread over the surface at 620°C, even when much of the chlorine is lost from the sample. Thus, the catalysts in Fig. 1 having Cl/Li <0.9 were relatively inactive because they had been calcined at 750°C, while the catalyst in Fig. 3a remained active after Cl/Li <0.9 because the temperature was kept below 620°C. This role of chlorine is enhanced by the fact that the surface areas were larger for the chlorided catalysts.

The effect of chlorine on C_2H_6 conversion was partially mimicked by decreasing the amount of lithium in a Li^+–MgO catalyst. For example, at constant space velocity in an integral reactor, conversions attained over the Li^+–MgO (0.030) and the Li^+–MgO (0.39) catalysts were 42 and 9%, respectively, after 10 h on stream. The ratio of conversions reflect the five-fold greater surface area of the Li^+–MgO (0.030) catalyst (Table 1), but such a comparison based on surface areas may be an oversimplification as the surface compositions of these two catalysts were quite different (see below).

Effect of CO_2 on activity and selectivity. It has been demonstrated previously that CO_2 has a major effect on the catalytic properties of Li^+–MgO catalysts (6, 9). Because of the basic nature of the catalysts, CO_2 poisons active centers, for both CH_4 and C_2H_6 conversions, but it also enhances selectivity at a constant level of conversion (10). By contrast, incorporation of Cl^- ions at a Cl/Li ratio of ca. 0.9 resulted in a catalyst for CH_4 conversion which was unaffected by CO_2 (3). As shown by the results of Fig. 4, after 5 h on stream the addition of up to 25 Torr of CO_2 had no effect on the conversion of C_2H_6 over the Li^+–MgO–Cl^- (0.46/0.69) catalyst, but the same amount of CO_2 seriously poisoned the Li^+–MgO–Cl^- (0.36/0.22) and the Li^+–MgO (0.03) catalysts. With respect to the results of Fig. 3, it should be noted that CO_2 partially poisoned the Li^+–MgO–Cl^- (0.46/0.69) catalyst when the Cl/Li ratio fell below 0.9; e.g., after 15 h at a relatively high space velocity.

The consequences of CO_2 poisoning are manifested in several different ways, which makes a simple comparison of chlorided and nonchlorided catalysts difficult. In Table 3, the specific rates over four catalysts are compared. Over the Li^+–MgO (0.03) catalyst, the rate increased by more than a factor of 6 as the space velocity was increased from 0.23 to 10.4 s^{-1}. This increase in rate is attributed to a lower partial pressure of CO_2 product over the catalysts at the larger space velocity. For the Li^+–MgO (0.03) catalyst the CO_2 pressure, due to the reaction, increased from 8.8 Torr at a SV = 10.4 s^{-1} to 65.1 Torr at a SV = 0.23 s^{-1}, which is greater than the range of partial pressures depicted in Fig. 4. The effect of space velocity on rate was much smaller over the Li^+–MgO–Cl^- (0.46/0.69) catalyst. In fact, one would not expect CO_2 to have any effect on rate. The smaller rates at the low space velocities may, in part, result from the fact that conversions were beyond the differential range. It is probably fortuitous that the Li^+–MgO–Cl^- (0.46/0.69) and the Li^+–MgO (0.03) catalysts had similar rates at a SV = 10.4 s^{-1}. At the larger space velocities, the activity of the Li^+–MgO–Cl^- (0.36/0.22) catalyst, having a Cl/Li ratio of 0.65 after calcination, was intermediate between that of a fully chlorided catalyst and one without chlorine.

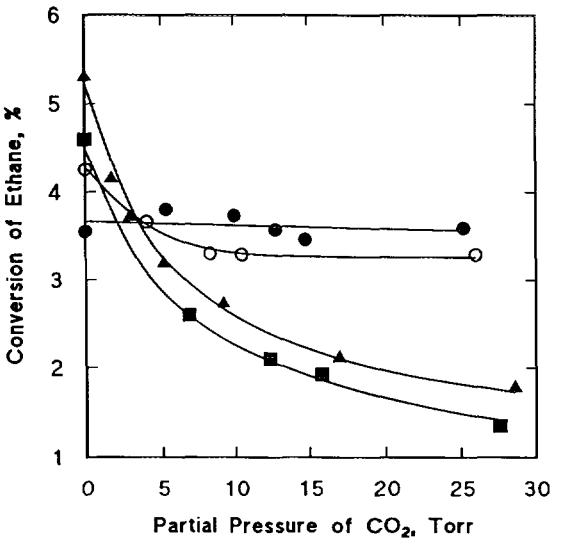

FIG. 4. Effect of CO_2 added to the reagents on the conversion of ethane: ●, Li^+–MgO–Cl^- (0.46/0.69) (0.2 ml) after 5 h on stream; ○, Li^+–MgO–Cl^- (0.46/0.69) after 15 h on stream; △, Li^+–MgO–Cl^- (0.36/0.22) (1.0 ml) after 175 h on stream; ■, Li^+–MgO (0.03) (0.05 ml). The amount of catalyst in the differential reactor was adjusted to give comparable C_2H_6 conversion in the absence of added CO_2. $P(C_2H_6)$ = 290 Torr, $P(O_2)$ = 290 Torr, T = 620°C, total flow rate = 60 ml/min.

Moreover, the effect of CO_2 is evident in the selectivities obtained over the four catalysts in Table 3. As indicated by the numbers in parentheses, only the Li^+–MgO–Cl^- (0.46/0.69) catalyst produced C_2H_4 selectivities >80% at the larger space velocities. The lower C_2H_4 selectivities obtained over the other catalysts reflect the fact that CO_2 is not available to poison the nonselective sites at the larger space velocities. The high C_2H_4 selec-

TABLE 3

Effect of Space Velocity on the Specific Activity

Catalyst	Space velocity (s^{-1})[a]					
	0.23[b]	1.1	2.2	4.3	5.2	10.4
Li^+–MgO–Cl^- (0.46/0.69)	2.2[c] (78)[d]	3.0 (77)			3.5 (86)	3.5 (88)
Li^+–MgO–Cl^- (0.36/0.22)	0.43 (75)	0.42 (74)			0.84 (79)	
Li^+–MgO (0.39)	0.53 (63)	0.68 (76)				1.1 (66)
Li^+–MgO (0.03)	0.57 (67)	1.4 (73)	2.1 (73)	2.9 (72)		3.9 (67)

[a] Space velocity changed by varying the amount of catalyst.
[b] Data obtained in the integral reactor.
[c] Specific activity (μmol/m^2/s).
[d] Selectivity to ethylene.

tivity obtained over the Li^+–MgO–Cl^- (0.46/0.69) catalyst implies that Cl^- ions similarly poison nonselective sites which are effective in the further oxidation of C_2H_4 to CO_x.

The C_2H_6 conversions and C_2H_4 selectivities as a function of temperature are shown in Fig. 5 for the same four catalysts. The corresponding activation energies are given in Table 4. Although it is not obvious from the data of Fig. 5, the relationship between conversion level and temperature is strongly affected by the presence of CO_2 for the catalysts Li^+–MgO–Cl^- (0.36/0.22), Li^+–MgO (0.03) and Li^+–MgO (0.39). This relationship is complex, however, because as the temperature increases, the conversion level and the selectivity both increase, as shown in Fig. 5b. The latter occurs because of the positive effect that CO_2 has on selectivity. In addition, CO_2 functions in a classical sense as a product which is also a poison. This results in the relationship

$$E_a = E + \lambda, \qquad [1]$$

where E_a is the apparent activation energy, E is the activation energy in the absence of the poison, and λ is the heat of adsorption of CO_2. The effect of CO_2 on the activation energy for CH_4 conversion over Li^+–MgO was previously demonstrated (6), and as part of this study we have shown that over the Li^+–MgO–Cl^- (0.36/0.22) catalyst, used for 400 h, E_a increased from 32 to 39 kcal/mol as the amount of CO_2 added to the system was increased from 2 to 8 Torr.

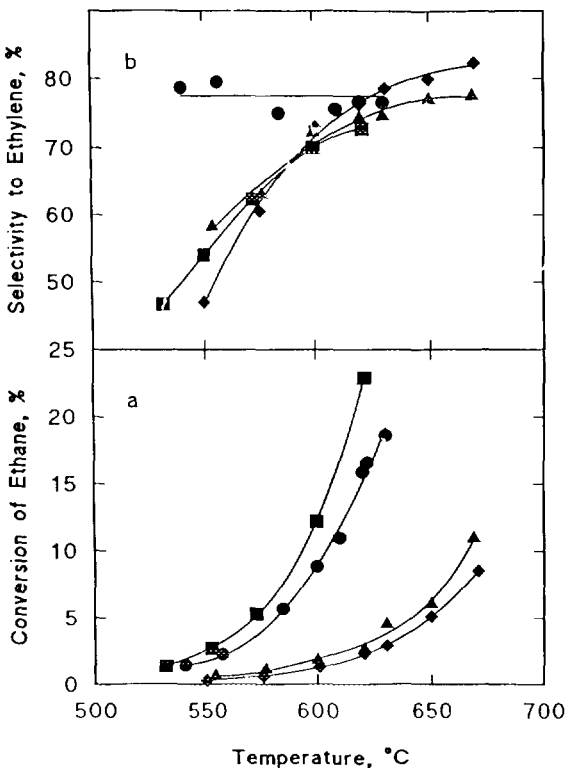

FIG. 5. Effect of temperature on (a) ethane conversion and (b) ethylene selectivity: ●, Li^+–MgO–Cl (0.46/0.69); △, Li^+–MgO–Cl^- (0.36/0.22); ■, Li^+–MgO (0.030); ◆, Li^+–MgO (0.39). $P(C_2H_6)$ = 290 Torr, $P(O_2)$ = 290 Torr. Data were taken with 1.0 ml catalyst after ca. 5 h on stream.

TABLE 4

Activation Energy for Ethane OXD[a]

Catalyst	E_a (kcal/mol)
Li^+–MgO–Cl^- (0.46/0.69)	43
Li^+–MgO–Cl^- (0.36/0.22)	33, 44[b]
Li^+–MgO (0.39)	44
Li^+–MgO (0.03)	45

[a] Activation energies obtained in differential reactor; total flow rate = 60 ml/min.

[b] A change in E_a was observed at ca. 620°C; the larger E_a corresponding to higher temperatures.

The increasing or constant C_2H_4 selectivity with increasing C_2H_6 conversion is unusual in heterogeneous catalysis. The increasing selectivity for catalysts with Cl/Li <0.9 can be adequately explained by the effect of CO_2, as described above. The CO_2 partial pressures increased with increasing conversion level, and the nonselective sites became poisoned. For the Li^+–MgO–Cl^- (0.46/0.69) catalyst, however, these nonselective sites had already been poisoned by Cl^- ions, and no additional effect resulted from the increased level of CO_2. We previously demonstrated, using ^{13}C-labeled reagents, that ethylene, rather than ethane, is the major source of CO_2 when the partial pressures of the hydrocarbons are comparable (11).

Kinetics of the reaction. Because CO_2, a product of the reaction, does not poison the Li^+–MgO–Cl^- catalysts having Cl/Li ≥0.9, the kinetics over these materials may be obtained in a straightforward manner. At 620°C, the reaction orders for Li^+–MgO–Cl^- (0.46/0.69) were 0.59 with respect to C_2H_6 and 0.30 with respect to O_2. At the same temperature, the corresponding orders over Li^+–MgO (0.03) were 0.58 and 0.18, respectively. The decrease in the order with respect to oxygen may reflect, in part, the poisoning effect of CO_2 for the Li^+–MgO catalyst as the partial pressure of O_2 increased.

As previously discussed for the OXD of ethane over Li^+–MgO, and by analogy with our mechanism for the oxidative coupling of methane, we propose that the alkane is activated by the abstraction of a hydrogen atom at a reactive oxygen ion at the surface (1, 3). This is followed by the rapid loss of water and the replacement of

lost lattice oxygen by O_2. A model developed for the oxidative coupling reaction suggests that the rate of active oxygen formation and decomposition, relative to the rate of hydrogen atom abstraction, determines the orders of reaction (3). Thus, the reaction order will depend on the C–H bond energy strength, which is different for CH_4 and C_2H_6, although the overall mechanism for alkane activation is the same. For example, over a Li^+–MgO–Cl^- catalyst the orders of reaction with respect to CH_4 and O_2 were 0.79 and 0.61, respectively. The small orders with respect to O_2 (0.58 and 0.18) indicate that the incorporation of oxygen is faster than the activation of C_2H_6; however, it is difficult to understand how the orders with respect to O_2 and C_2H_6 can *both* be so small. This suggests that another process, such as oxygen mobility in the lattice, may approach a rate-limiting condition.

The potential role of gas-phase chlorine. Since Cl atoms are known to serve as chain carriers in the homogeneous dehydrogenation of ethane, it has been suggested that gas-phase chlorine, derived from the catalyst, may also play a role in the OXD reaction (12, 13). This subject has been addressed in detail with respect to the formation of C_2H_4 during the oxidative coupling of CH_4. Perhaps the most definitive evidence against a substantial gas-phase component is found in the recent transient studies of Burch *et al.* (14). They observed that the positive effect of chlorine addition to a MgO catalyst persisted long after the flow of CH_3Cl over the catalyst had ceased. Earlier, Conway and Lunsford (1) had shown that there was no correlation between the rate of chlorine loss from an Li^+–MgO–Cl^- catalyst and its OXD activity.

The results of Table 2 further support the role of a surface chlorine species, rather than gas-phase chlorine, in promoting the OXD of ethane. Again, there was no correlation between the rate of chlorine evolution from the catalyst and the conversion of C_2H_6. For example, with the Li^+–MgO–Cl^- (0.46/0.69) catalyst, the conversion increased from 68 to 72% while the rate of chlorine evolution decreased from 244 to 100 μmol/h. Moreover, integrated C_2H_4/Cl ratios (i.e., the molecules of C_2H_4 formed per molecule of Cl released from the catalyst) ranged from 223 to 614. These values indicate excessively long chain lengths if Cl-initiated homogeneous reactions were responsible for the C_2H_6 conversion. As reported previously (1), the addition of H_2O to the reagents caused an increase in the rate of chlorine evolution as HCl. The addition of water to the rather inactive Li^+–MgO–Cl^- (0.36/0.22) catalyst caused a 12-fold increase in the rate of Cl evolution, but almost no change in the C_2H_6 conversion.

The effect of gas-phase HCl was further demonstrated in a temporal experiment, the results of which are depicted in Fig. 6. At the outset, the rate of C_2H_4 formation

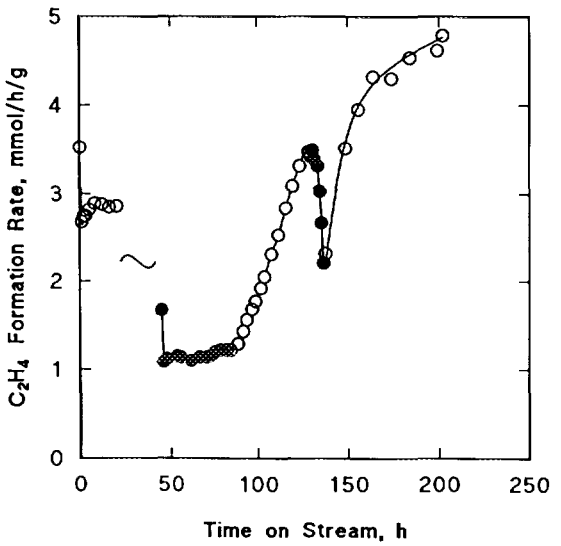

FIG. 6. Response of ethylene formation to the addition of HCl in the gas stream over a Li^+–MgO (0.24) catalyst: (○) no HCl added; (~) sample exposed to 1% HCl in He; (●) 180 Torr of 1% HCl in He added to reaction mixture. $P(C_2H_6)$ = 290 Torr, $P(O_2)$ = 290 Torr, T = 650°C, total flow rate = 60 ml/min, 5.4 g catalyst.

was first determined over a Li^+–MgO catalyst. Then after 21 h, the reagent flow was stopped and a gas mixture of 1% HCl in He was passed over the catalyst for 24 h. Upon introducing C_2H_6 and O_2 along with the HCl/He mixture, it was found that the modified catalyst was less active than the catalyst without chlorine. Only when the flow of HCl was stopped did the activity increase, and it decreased again when the HCl was readmitted. Finally, when the HCl was turned off a second time, the activity increased considerably beyond the original level. These results demonstrate that (i) gas-phase chlorine at a level of 1.8 Torr had a negative effect on C_2H_4 formation, (ii) excess chlorine on the surface resulted in a lower activity, and (iii) as excess chlorine was lost from the catalyst, higher levels of activity were attained. The second point is consistent with the results of Fig. 2a, which showed that the activity of the Li^+–MgO–Cl^- (0.46/0.69) catalyst actually increased with time on stream.

Temperature-programmed desorption. From the TPD spectra of Fig. 7 it is evident that the catalysts in various stages of use contain several different types of CO_2 adsorption sites. Here we use the term "adsorption" to include surface carbonates, since XPS results (see below) indicate that much, if not all, of the CO_2 is held on the surface in this form. The previous study of freshly calcined catalysts demonstrated that as the Cl/Li ratio decreased from 0.9 to 0, the amount of CO_2 adsorbed and the number of adsorption states increased (3). The focus of the present study was to determine how the adsorption

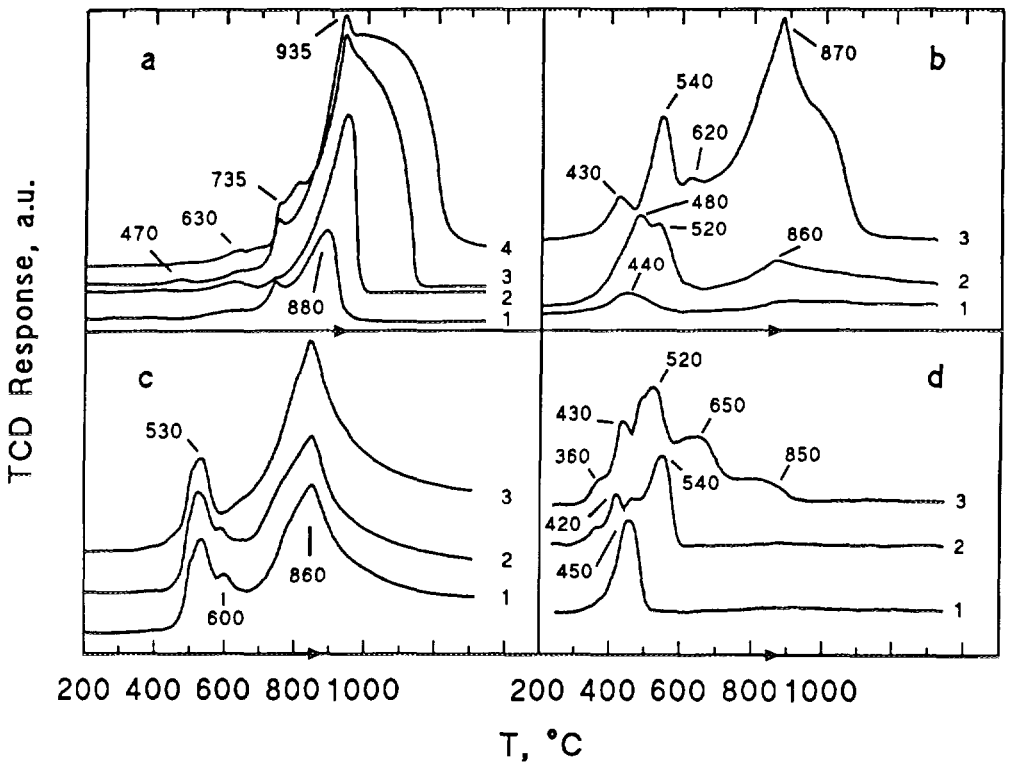

FIG. 7. TPD curves for CO_2 desorbing from catalysts. (a) Li^+–MgO (0.03), curve 1; Li^+–MgO (0.06), curve 2; Li^+–MgO (0.13), curve 3; Li^+–MgO (0.29), curve 4. (b) Li^+–MgO–Cl (0.46/0.69), curve 1, fresh catalyst; curve 2, used 5 h; curve 3, used 250 h. (c) Li^+–MgO–Cl (0.36/0.22), curve 1, fresh catalyst; curve 2, used 5 h; curve 3, used 400 h. (d) Li^+–MgO–Cl^- (0.34/0.34), curve 1, fresh catalyst; curve 2, used 13 h; curve 3, used 550 h.

states of the Li^+–MgO–Cl^- catalysts evolved during the course of the OXD reaction. As a point of reference, the CO_2 TPD curves for four fresh Li^+–MgO catalysts containing different amounts of Li are shown in Fig. 7a. With an increasing concentration of lithium, the amount of adsorbed CO_2 increased, and, moreover, the temperature corresponding to the maximum desorption rate increased. For example, the temperature for this maximum shifted from 880°C for Li^+–MgO (0.03) to 935°C for Li^+–MgO (0.39). This is taken as evidence that the less basic MgO interacts with more basic Li_2O, and the influence of MgO on the Li_2O is greater when the Li/Mg ratio is small.

As shown in Fig. 7b, curve 1, the calcined, but fresh Li^+–MgO–Cl^- (0.46/0.69) catalyst exhibited a small CO_2 desorption peak at 440°C and a slight increase in desorption at about 850°C, but essentially no desorption occurred between 600 and 800°C. This result is consistent with the observation that the fresh Li^+–MgO–Cl^- (0.46/0.69) catalyst was not poisoned by CO_2 during the OXD reaction. After 5 h on stream (curve 2), a new peak was observed at 520°C, and additional CO_2 desorption occurred over the range between 500 and 800°C. The presence of these sites for CO_2 adsorption is surprising in view of the small amount of chlorine that was lost from the surface over this time period (Fig. 3). XPS results (see below) confirm that CO_3^{2-} ions were present on this material. Since the catalyst at this stage was not poisoned, the state of CO_2 monitored by TPD is apparently not related to the activation of C_2H_6. After 250 h on stream, we know that most of the chlorine had been lost from this catalyst (Fig. 3). In the temperature range of interest, the peak at 520°C shifted to 540°C (curve 3), a new peak appeared at 620°C, and increasing CO_2 desorption was observed as the temperature increased. The reversible CO_2 poisoning effect on this catalyst is consistent with the peak at 620°C and the increasing CO_2 desorption.

By contrast, after calcination the Li^+–MgO–Cl^- (0.36/0.22) catalyst had TPD peaks at ca. 530 and 600°C, and a large CO_2 background that increased up to 860°C (Fig. 7c). This behavior is consistent with the catalytic results of Figs. 4 and 5, which show that this catalyst was similar to a Li^+–MgO catalyst.

The CO_2 TPD from the Li^+–MgO–Cl^- (0.34/0.34) catalyst, which was prepared by the addition of LiCl, is given in Fig. 7d. The TPD curve of the fresh sample is similar to that obtained over the Li^+–MgO–Cl^- (0.46/0.69) catalyst (Fig. 7b, curve 1) except that the peak at 450°C is some-

what larger. After 13 h in the *integral* reactor, which corresponds to the time required for maximum activity, the peak at 540°C dominated the spectrum, and above 600°C there was almost no CO_2 desorption (curve 2). After 550 h on stream, high-temperature maxima were observed at 520, 650, and ca. 850°C. Although the temperatures corresponding to the peak maxima are similar, the relative amplitudes are different from those obtained with a Li^+–MgO sample. In particular, with the Li^+–MgO–Cl^- (0.34/0.34) catalyst, the amount of the most strongly held CO_2 was substantially less. Clearly, the amount and the method of chloride addition affect the distribution of strongly basic sites that evolve as chlorine is lost from the surface during the OXD reaction.

Composition of the near-surface region. The most definitive evidence for the role of chlorine in Li^+–MgO–Cl^- catalysts comes from XPS results. The binding energies for Li, Mg, C, O, and Cl obtained with pure compounds and catalyst samples are reported in Table 5. The binding energies of the pure compounds are in good agreement with those given in the literature (15). Although the Li(1s) binding energies are similar, in LiCl the binding energy is consistently 0.6–1.2 eV greater than for the other compounds of lithium. Thus, as shown in Fig 8, spectrum b, it is possible to estimate the atomic percentage of lithium that is present as the chloride. Although lithium has a relatively small XPS cross section, one can easily detect its presence, even in the Li^+–MgO (0.03) sample. Similarly, since the binding energies of carbon in the carbonate ion and in adventitious carbon differ by about 5 eV, one can estimate from the C (1s) signals the fraction of Li_2CO_3 on the surface. $MgCO_3$ decomposes at about 400°C, and therefore would not be present on the surface, except for those samples that were cooled in CO_2. Although we will refer to the surface compound generically as Li_2CO_3, one should keep in mind the TPD results which indicate that the carbonates exist in several states. Only one form of chlorine was

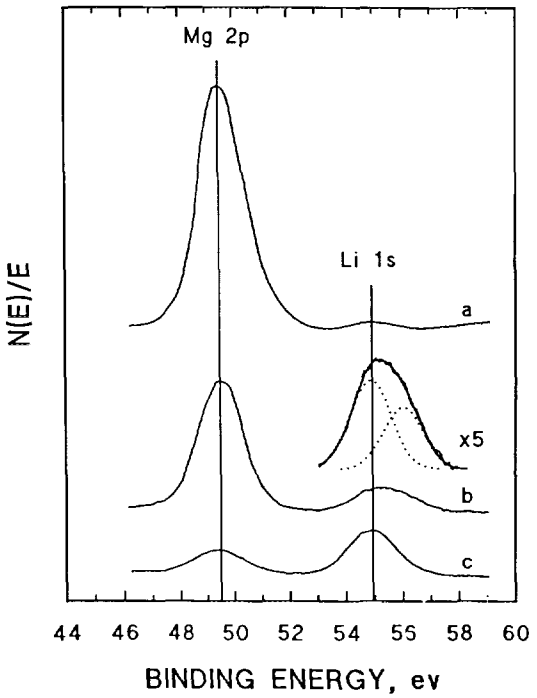

FIG. 8. X-ray photoelectron spectra of fresh catalysts in the Mg(2p) and Li(1s) BE region: (a) Li^+–MgO (0.03); (b) Li^+–MgO–Cl (0.36/0.22); (c) Li^+–MgO (0.39).

TABLE 5

Binding Energies of Pure Compounds and Catalysts

Sample	Binding energies (ev)							
	Li(1s)			C(1s)		O(1s)		
	Cl	CO_3^{2-}, O^{2-}, OH	Mg(2p)	Adv.	CO_3^{2-}	O^{2-}	CO_3^{2-}, OH^-	Cl(2p)
Li_2CO_3		55.3		284.6	289.9		531.4	
LiCl	55.9			284.6	288.9		531.1	198.4
MgO			49.1	284.6	289.0	529.0	531.1	
Li^+–MgO (0.03)		54.8	48.9	284.6	289.1	528.9	531.1	
Li^+–MgO (0.39)		55.2	49.7	284.6	289.8		531.4	
Li^+–MgO–Cl (0.46/0.69)[a]	56.2		49.6	284.6	289.2	529.7	531.6	198.7
Li^+–MgO–Cl (0.46/0.69)[b]	56.0	54.9	49.2	284.6	288.8	529.3	531.5	198.6
Li^+–MgO–Cl^- (0.36/0.22)[a]	56.0	54.9	49.3	284.6	289.6	529.3	531.2	198.4
Li^+–MgO–Cl^- (0.36/0.22)[b]	56.0	54.9	49.2	284.6	289.0	529.3	531.2	198.6

[a] Calcined sample (see Experimental) removed from bottle in a glove box, pressed into a wafer, and transferred to the XPS instrument in a sealed vessel.

[b] After use in differential reactor ca. 14 h, catalyst was cooled rapidly in flowing O_2/He/CO_2 (10–20 Torr). The wafer was prepared in the glove box and transferred to the XPS instrument in a sealed vessel.

found on the catalysts and the binding energy corresponds to that of Cl^- ions.

The surface compositions of the pure compounds and selected catalysts are given in Table 6. The surface compositions of the pure compounds are consistent with those expected from bulk compositions. For the MgO sample, which was not pretreated at elevated temperatures, it is evident that two types of oxygen are present: one with BE = 529.0 eV is attributed to O^{2-} ions and the other at BE = 531.4 eV is mainly present as OH^- ions. The O(1s) binding energy in carbonate ions also occurs at 531 eV, but it is evident from the results for MgO that there was relatively little carbonate on the surface.

The surface compositions of the two Li^+–MgO samples used in this study are compared in Table 6. As noted by other investigators (16, 17), when the lithium content is large (Li^+–MgO (0.39)), the surface is mainly covered by a Li_2CO_3 phase. This is demonstrated in Fig. 8. spectrum c, by the reduction in the amount of Mg at the surface and presence of a large percentage of lithium carbonate ions. The ratio of Li, C, and O is approximately that expected for Li_2CO_3. Following its use for 40 h, the amount of Li_2CO_3 decreased, and more MgO appeared on the surface. Even at a relatively low reaction temperature of 620°C, lithium is slowly lost from the surface.

By contrast, the surface of the more active Li^+–MgO (0.03) catalyst consisted mainly of MgO, although a small amount of lithium was also present. The amount of oxygen having a binding energy of 531 eV is too large for it to be only carbonate oxygen, based on the Li (1s) and the C(1s) (carbonate) signals. This oxygen probably results from OH^- ions on the surface, although O^- and O_2^{2-} ions may also contribute (17, 18).

The XPS study of the chlorided catalysts focused on the Li^+–MgO–Cl^- (0.46/0.69) and Li^+–MgO–Cl^- (0.36/0.22) samples, both of which had a large amount of lithium. It is evident from the results of Table 6 that the Li^+–MgO–Cl^- (0.46/0.69) samples calcined in air had mainly LiCl and MgO on the surface; i.e., there was very little Li_2CO_3 present. Oxygen may have been present as OH^-, O_2^{2-}, or O^- ions. After 14 h in the differential reactor, a small amount of Li_2CO_3 began to appear on the Li^+–MgO–Cl^- (0.46/0.69) catalyst, but the surface remained mainly MgO. This was the case even when the catalyst was cooled in a gas mixture that contained CO_2.

Qualitatively, the XPS data, which are in agreement with the TPD results, help one understand the specific activities of the Li^+–MgO (0.39), Li^+–MgO (0.03), and Li^+–MgO–Cl^- (0.46/0.69) catalysts reported in Table 3. Li^+–MgO (0.39) was extensively covered by a relatively inactive film of Li_2CO_3/Li_2O. The coverage of Li_2CO_3 was much less extensive on the Li^+–MgO (0.03) sample, but it contained more than was found on the fresh Li^+–MgO–Cl^- (0.46/0.69) sample.

Similarly, the XPS results for the Li^+–MgO–Cl^- (0.46/0.69) and Li^+–MgO–Cl^- (0.36/0.22) samples are consistent with the catalytic data of Fig. 3. The fresh Li^+–MgO–Cl^- (0.36/0.22) catalyst was about half covered with $LiCl/Li_2CO_3/Li_2O$, which is reflected by its lower activity, but the extent of the decrease in activity is greater than might be expected from a merely physical blocking of the MgO surface. After use as a catalyst for 14 h the Li^+–MgO–Cl^- (0.46/0.69) catalyst had only a small amount of Li_2CO_3 on the surface, and from the TPD results (Fig. 7b) most of this was in a thermally unstable form. By contrast, the Li^+–MgO–Cl^- (0.36/0.22) catalyst

TABLE 6

Surface Composition of Pure Compounds and Catalysts

	Surface composition (atom%)							
	Li(1s)			C(1s)		O(1s)		
Sample	Cl^-	CO_3^{2-}, O^{2-}, OH^-	Mg(2p)	Adv.	CO_3^{2-}	O^{2-}	CO_3^{2-}, OH^-	Cl(2p)
Li_2CO_3		32			16		52	
LiCl	45			18				37
MgO			32	14	3	27	24	
Li^+–MgO (0.03)		2	30	13	4	31	20	
Li^+–MgO (0.39)		24	2	11	15		48	
Li^+–MgO–Cl^- (0.46/0.69)[a]	4		26	16	2	3	16	5
Li^+–MgO–Cl^- (0.46/0.69)[b]	7	2	19	16	3	24	21	9
Li^+–MgO–Cl^- (0.36/0.22)[a]	7	11	13	10	5	17	28	9
Li^+–MgO–Cl^- (0.36/0.22)[b]	8	8	14	16	5	16	24	9

[a] Calcined sample (see Experimental) removed from bottle in a glove box, pressed into a wafer, and transferred to the XPS instrument in a sealed vessel.

[b] After use in differential reactor ca. 14 h, catalyst was cooled rapidly in flowing $O_2/He/CO_2$ (10–20 Torr). The wafer was prepared in the glove box and transferred to the XPS instrument in a sealed vessel.

had less surface Li_2CO_3 after 5 and 12 h of use than did the fresh catalyst. Moreover, the amount of MgO available at the surface increased. These results are consistent with the slow increase in C_2H_6 conversion that was indicated in Fig. 3b. A loss of Li_2CO_3 from the catalysts is not reflected in the TPD results of Fig. 7c, which suggests that during reaction there may be the transformation from a Li_2CO_3 film to crystallites with time on stream.

MODEL OF THE ACTIVE SURFACE

The results presented here can be interpreted in terms of a model of the catalytic surface described in Scheme 1. When the Cl/Li ratio is ≥ 0.9, most of the lithium is present as molten LiCl, (m.p. = 613°C) rather than as Li_2CO_3. The XPS results indicate that LiCl does not spread over the MgO surface. Although LiCl itself is not active for the OXD of ethane, it favorably influences the activity in three ways: (i) it inhibits the sintering of the catalyst by Li_2CO_3, (ii) it prevents Li_2CO_3 from covering the catalyst, and (iii) it stabilizes the form of lithium which activates oxygen, but does not strongly interact with CO_2. We suggest that this active form of lithium may be described by **I**. In **I**, atomic layers of Li_2O decorate the surface of the molten LiCl, and the basicity of the oxygen is modified to the extent that a surface carbonate is not formed under reaction conditions. The solubility of Li_2O in LiCl is only 1.1% at 650°C (18). From a separate set of pulse reaction experiments, we have demonstrated that fresh Li_2O has comparable activity, but somewhat less C_2H_4 selectivity, than a good Li^+–MgO–Cl^- catalyst. Here we ascribe the activity to Li_2O, but it may, in fact, be due to special forms of oxygen (e.g., O^- or O_2^{2-} ions). As noted previously (3), the centers that are principally responsible for the activation of C_2H_6 may not be the same as those that are responsible for the activation of CH_4.

Only a very limited amount of Li_2O can be supported in a single atomic layer, and when the Cl/Li ratio is <0.8, multilayers of Li_2O form. In the presence of air or the reaction mixture, the Li_2O becomes Li_2CO_3, part of which forms a eutectic mixture with LiCl (19). Pretreatment of the catalyst at 750°C in air, which contains H_2O and CO_2, causes the Li_2CO_3 and the LiCl/Li_2CO_3 to flow extensively onto the MgO as described by **II**, but if the Li_2CO_3 is formed under reaction conditions at 620°C, it is not as well dispersed.

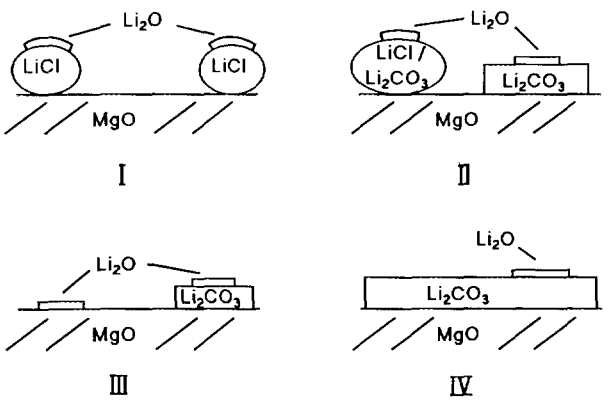

SCHEME 1

As shown in Table 3 and Fig. 4, high OXD activity, but not the resistance to CO_2 poisoning, can be achieved by adding only a small amount of lithium to magnesium oxide. If all of the lithium in the Li–MgO (0.03) catalyst were present as Li_2CO_3 the equivalent monolayer coverage would be 2. In this case, described by **III**, the Li_2O is believed to be highly dispersed and the influence of the less basic MgO substrate partially inhibits the formation of Li_2CO_3. This effect is evident in the TPD results of Fig. 7a, which show that at the smaller Li loading the fraction of CO_2 desorbing at lower temperatures increased. We have demonstrated for the BaO/MgO catalyst that at low loadings of Ba the MgO can substantially reduce the basicity of the BaO, while still maintaining good activity for CH_4 conversion (20).

For the Li–MgO (0.39) catalyst, the uniform coverage of Li_2CO_3 would be equivalent to 160 monolayers. Under reaction conditions, Li_2CO_3 would be favored, and only a relatively small amount of Li_2O would be present on the surface, as described by **IV**, for the activation of C_2H_6.

The behavior of the Li^+–MgO–Cl^- (0.46/0.69) catalyst, as described in Fig. 3, may now be more fully understood in view of this model. As the chlorine is lost from the sample at 620°C, the Li_2CO_3 remains mainly in the LiCl/Li_2CO_3 phase, although some of it migrates to the MgO where there is an equilibrium between dispersed Li_2O and Li_2CO_3. Thus, the state of the catalyst is intermediate between **I** and **II**. The catalyst remains active, but it is subject to poisoning by CO_2. In general, a highly basic catalyst intrinsically is more effective in activating an alkane, but it is also extensively poisoned by CO_2. Therefore, under steady-state conditions a less basic catalyst may be more active, particularly with respect to C_2H_6 which has a weaker C–H bond than CH_4.

ACKNOWLEDGMENT

This research was supported by the Gas Research Institute under Contract 5086-260-1326.

REFERENCES

1. Conway, S. J., and Lunsford, J. H., *J. Catal.* **131,** 513 (1991).
2. Hinson, P. G., Clearfield, A., and Lunsford, J. H., *J. Chem. Soc., Chem. Commun.*, 1430 (1991).
3. Lunsford, J. H., Hinson, P. G., Rosynek, M. P., Shi, C., Xu, M., and Yang, X., *J. Catal.* **147,** 301 (1994).

4. Burch, R., and Crabb, E. M., *Appl. Catal. A: General* **97,** 49 (1993).
5. Conway, S. J., Wang, D. J., and Lunsford, J. H., *Appl. Catal. A: General* **79,** L1 (1991).
6. Xu, M., Shi, C., Yang, X., Rosynek, M. P., and Lunsford, J. H., *J. Phys. Chem.* **96,** 6395 (1992).
7. Baldwin, T. R., Burch, R., Crabb, E. M., Squire, G. D., and Tsang, S. C., *Appl. Catal.* **56,** 219 (1989).
8. Conway, S. J., Szanyi, J., and Lunsford, J. H., *Appl. Catal.* **56,** 149 (1989).
9. Korf, S. J., Roos, J. A., deBruijn, N. A., van Ommen, J. G., and Ross, J. R. H., *J. Chem. Soc., Chem. Commun.,* 1443 (1987).
10. Wang, D., Xu, M., Shi, C., and Lunsford, J. H., *Catal. Lett.* **18,** 323 (1993).
11. Shi, C., Rosynek, M. P., and Lunsford, J. H., *J. Phys. Chem.* **98,** 8371 (1994).
12. Ahmed, S., and Moffat, J. B., *Appl. Catal.* **58,** 83 (1990).
13. Warren, B. K., *Catal. Today* **13,** 311 (1992).
14. Burch, R., Chalker, S., and Hibble, S. J., *Appl. Catal. A: General* **96,** 289 (1993); Burch, R., Chalker, S., and Loader, P. *in* "New Frontiers in Catalysis" (L. Guczi, F. Solymosi, and P. Tetenyi, Eds.), pp. 1079–1092. Elsevier, Amsterdam.
15. Contour, J. P., Salesse, A., Froment, M., Garreau, M., Thevenin, J. and Warin, D., *J. Microsc. Spectrosc. Electron* **4,** 483 (1979); Morgan, W. E., Van Wazer, J. R., and Stec., W. J., *J. Am. Chem. Soc.* **95,** 751 (1973); Inoue, Y., and Yasumori, I., *Bull. Chem. Soc. Jpn.* **54,** 1505 (1981); Nefedov, V. I., Firsov, M. N. and Shaplygin, I. S., *J. Electron Spectrosc. Relat. Phenom.* **26,** 65 (1982); Nefedov, V. I., Gati, D., Dzhurinskii, B. F., Sergushin, N. P., and Salyn, Y. V., *Zh. Neorg. Khim.* **20,** 2307 (1975).
16. Miradatos, C., Martin, G. A., Bertolini, J. C., and Saint-Just, J., *Catal. Today* **4,** 301 (1989).
17. Peng, X. D., Richards, D. A., and Stair, P. C., *J. Catal.* **121,** 99 (1990).
18. Nakajima, T., Nakanishi, K., and Watanabe, N., *Nippon Kagaku Kaishi,* 617 (1975); *Bull. Chem. Soc. Jpn.* **49,** 994 (1976).
19. Dessureault, Y., Sangster, J., and Pelton, A. D., *J. Phys. Chem. Ref. Data* **19,** 1164 (1990).
20. Dissanayake, D., Lunsford, J. H., and Rosynek, M. P., *J. Catal.* **143,** 286 (1993).